



IRRADIANCE DISTRIBUTION OF IMAGE SURFACE IN MICROLENS ARRAY SOLAR CONCENTRATOR

Ali H. Al-Hamdani¹, Hayfa G. Rashid² and Alaa B. Hasan³

¹Department of Laser and Optoelectronics Engineering, University of Technology, Baghdad, Iraq

²College of Education, Al-Mustansiryia University, Baghdad, Iraq

³College of Education, University of Baghdad, Iraq

E-Mail: ali_alhamdani2003@yahoo.com

ABSTRACT

Irradiance distribution of image surface has been investigated in multiple prototypes of microlens array solar concentrator by using optical design program ZEMAX in sequential and nonsequential ray tracing mode. The prototypes composed of 1-D or 2-D acrylic microlens array with and without multimode slab waveguide to concentrate sun light in photovoltaic cell PVC. All optical concentrator systems ensure roughly organized power distribution in all photovoltaic cell (PVC).

Keywords: microlens array, irradiance distribution, waveguide, photovoltaic cell (PVC), total internal reflection (TIR).

INTRODUCTION

Irradiance is the power of electromagnetic radiation per unit area incident on a surface. The SI units for this quantities is (W/m²), this quantity is sometimes called intensity that characterize the total amount of radiation present, at all frequencies. If a point source radiates light uniformly in all directions through a non-absorptive medium, then the irradiance decreases in proportion to the square of the distance from the object. The irradiance of a monochromatic light wave in matter is given in terms of its electric field by [1]:

$$I \approx \frac{cnE_0}{2} |E|^2 \quad (1)$$

where E is the complex amplitude of the wave's electric field, n is the refractive index of the medium, c is the speed of light in vacuum, and ϵ_0 is the vacuum permittivity. (This formula assumes that the magnetic susceptibility is negligible, i.e., $\mu_r \approx 1$ where μ_r is the magnetic permeability of the light transmitting media. This assumption is typically valid in transparent media in the optical frequency range [2].

The global irradiance on a horizontal surface on Earth consists of the direct irradiance E_{dir} and diffuse irradiance E_{dif} . On a tilted plane, there is another irradiance component: E_{ref} , which is the component that is reflected from the ground. The average ground reflection is about 20% of the global irradiance. Hence, the irradiance E_{tilt} on a tilted plane consists of three components [3]:

$$E_{tilt} = E_{dir} + E_{dif} + E_{ref}$$

The integral of solar irradiance over a time period is solar irradiation or insolation. Irradiation is generally measured in J/m².

Previous work describes the practical measurement of diffuse, global and direct solar irradiance. The relationship of diffuse irradiance to the turbidity factor and solar elevation angle is examined. Important

concepts related to visibility are defined, and conclude by illuminating the relationship between measurements of diffuse solar irradiance on clear days and meteorological visibility [4].

Another work was investigated the global and diffuse solar radiation incident on solar cells is simulated using a spectral model, for varying atmospheric. The effect of changes in total intensity and spectral distribution on the short circuit current and efficiency of different kinds of thin film solar cells (CdTe, nc-Si:H and CIGS) is examined [5]. Experimental and theoretical design for a new array micro lens concentrator was done by alhamdani [6].

In this work, the irradiance distribution measured in ZEMAX as a function of radial field coordinate. Irradiance is defined as the intensity of irradiation per unit area of image surface normalized to the irradiation at the point in the field that has maximum irradiation [7]. The computations were carried on the following: apodization, vignetting, aperture diameter, aberrations, image surface shape, angle of incidence and polarization.

Optical system prototypes

In this work, there are many optical system prototypes have been used as a compact solar concentrator systems to evaluate irradiance distribution. Some of these are functionally appropriate to use sequential ray tracing mode, like one and two dimensions Plano-convex microlens array, where sunlight collected by each lens of the array to focus into small area of PVC.

Other prototypes are fit to work in non-sequential ray tracing mode, these prototypes composed of two dimensions Plano-convex micro lens array, low refractive index cladding material and slab waveguide, where sunlight collected by the array focuses onto localized prisms (facets) mirrors positioned in the bottom of slab to reflect light at angles that exceed the critical angle defined by Snell's law propagate via total internal reflection (TIR) within the waveguide to the exit aperture where PVC is fixed.



(1-D) and (2-D) Plano-convex micro lens array

One dimension microlens is characteristically composed of one plane surface and one spherical surface that are used to refract light. Acrylic microlens arrays are composed of several lenses (20x1) that form a one-dimensional array on (1mm) a supporting slice substrate. The design divides the upward-facing primary into several small apertures, each with its own individual secondary element and 20 solar cells.

While two dimension microlens is characteristically composed of Acrylic microlens arrays are composed of several lenses (20x20) that form a two-dimensional array on a supporting slice substrate. The design divides the upward-facing primary into several small apertures, each with its own individual secondary element and 400 solar cells. Figure-1 shows cross section of plano-convex microlens array associated with PVCs that supported by slice in 1-D and 2-D prototypes.

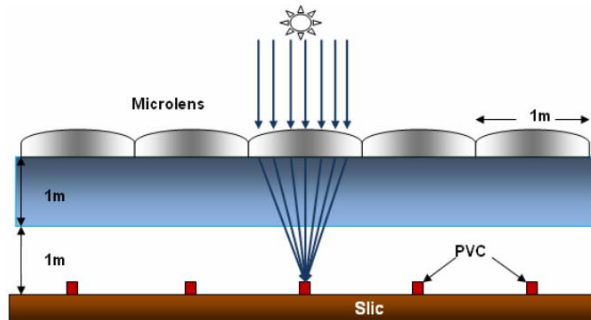


Figure-1. Cross section of 1-D and 2-D plano-convex microlens array.

(2-D) Plano-convex micro lens array with slab waveguide

An alternative approach for planar concentration has been investigated by replacing multiple non imaging secondary optics and their associated PVCs with a single BK7 glass waveguide (3mm) connected to a shared PVC, and (0.1 mm) air cladding between the array and slab. Sunlight collected by each aperture of the lenses array primary is coupled into a common slab waveguide using localized mirror prisms embedded on the backside of the waveguide to reorient focused light into guided modes that exceed the critical angle propagate via total internal reflection TIR within the waveguide to the exit aperture, typically at the edge of the slab. TIR is a complete reflection with negligible spectral or polarization-dependent losses which enables long propagation lifetimes. Guided rays can strike a subsequent coupling region and decouple as loss. The number of TIR interactions during propagation to the PVC affects the likelihood of decoupling and therefore the optical efficiency. Couplers typically cover (30% or 35%) of the waveguide surface enabling the system to yield both high efficiency and high concentration. The waveguide transports sunlight collected over the entire input aperture to single PVC placed at the waveguide edge. PVC alignment becomes trivial since comparatively large cells

are cemented to the waveguide edges. Fewer PVC's reduce connection complexity and allow one heat sink to manage the entire system output [8] as shown in Figure-2.

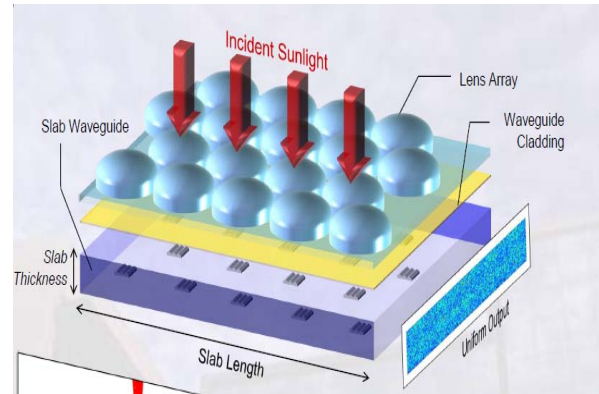


Figure-2. Plano-convex microlens array with slab waveguide [9].

Waveguide slab has two samples

Single ray propagation sample has asymmetrical prism angles equal to 60° , propagates rays in one way at edge of slab waveguide where PVC is fixed. Prisms reflect rays that collected by lenses with angle equals to 60° at upper surface of slab that exceed critical angle and satisfy TIR. This operation is repeating at other surfaces until reach at slab edge where PVC is fixed as shown in Figure-3.

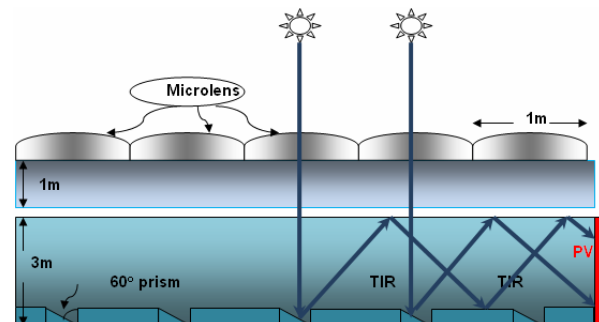


Figure-3. Cross section of plano-convex microlens array with slab waveguide; single ray propagation sample.

Double Ray Propagation Sample has symmetrical prism angles equal to 120° , propagates rays in two ways at edges of slab waveguide where PVCs are fixed. Prisms reflect rays that collected by lenses with angle equals to 60° at upper surface of slab that exceed critical angle and satisfy TIR. This operation is repeating at other surfaces until reach to slab edges where PVCs are fixed as shown in Figure-4.

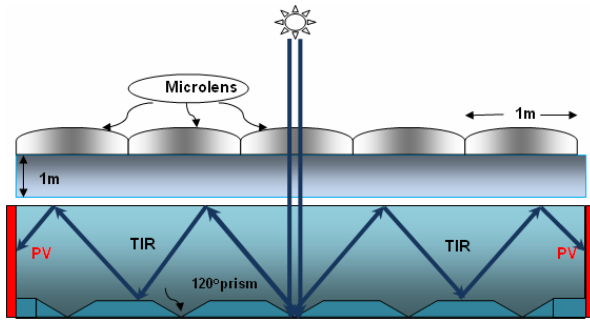


Figure-4. Cross section of plano convex microlens array with slab waveguide; double ray propagation sample.

RESULT AND DISCUSSIONS

In 1-D plano-convex microlens array prototype; Figure-5 shows irradiance distribution measured by sequential ray tracing mode in ZEMAX program at individual PVC which has most irradiance in radius 0.03mm. While Figures 6 and 7 shows the total irradiance distribution in overall slice at image surface 2-D and 3-D respectively. The system has peak irradiance of 15.66 W/mm², this number represents amount of total irradiance that incomes the image surface. Figure-4 shows slightly variation of irradiance distribution in the slice due to light diffraction. However, the optical system ensures roughly organized power distribution in all PVC's.

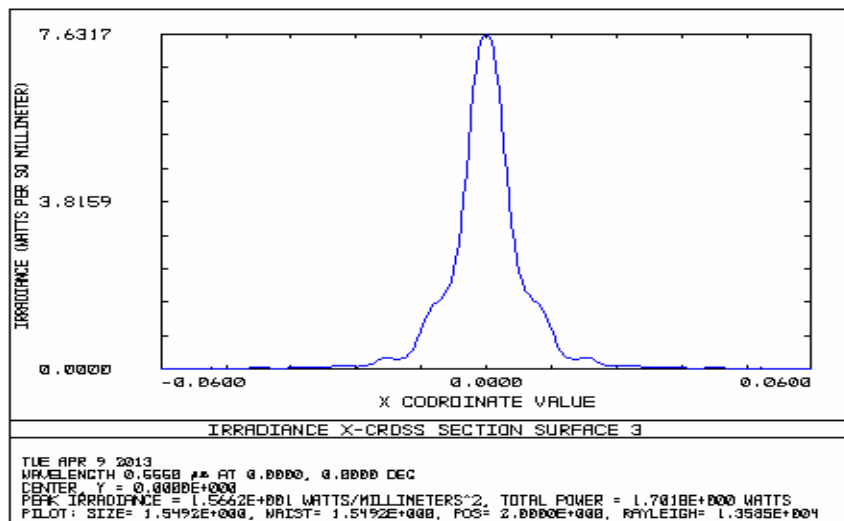


Figure-5. Irradiance distribution in image surface at individual PVC.

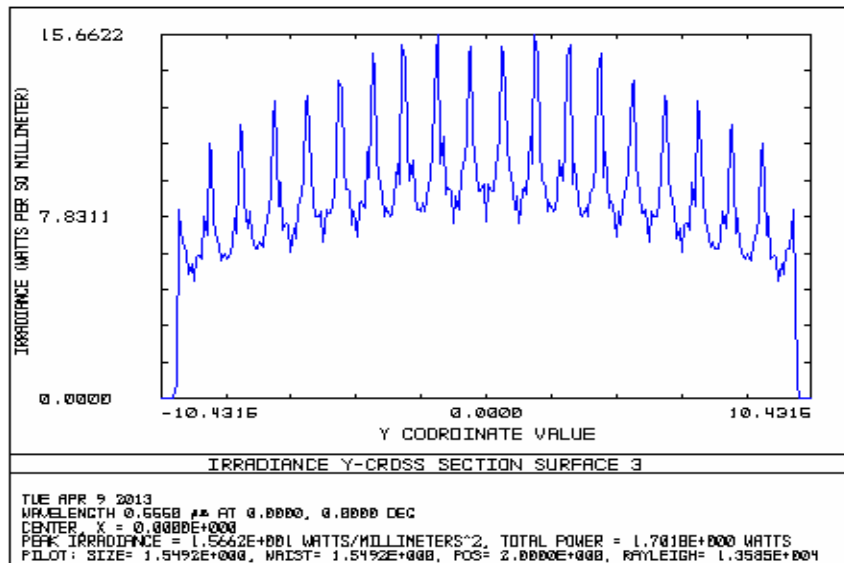


Figure-6. Y-cross Irradiance distribution in image surface at overall slice.



www.arnjournals.com

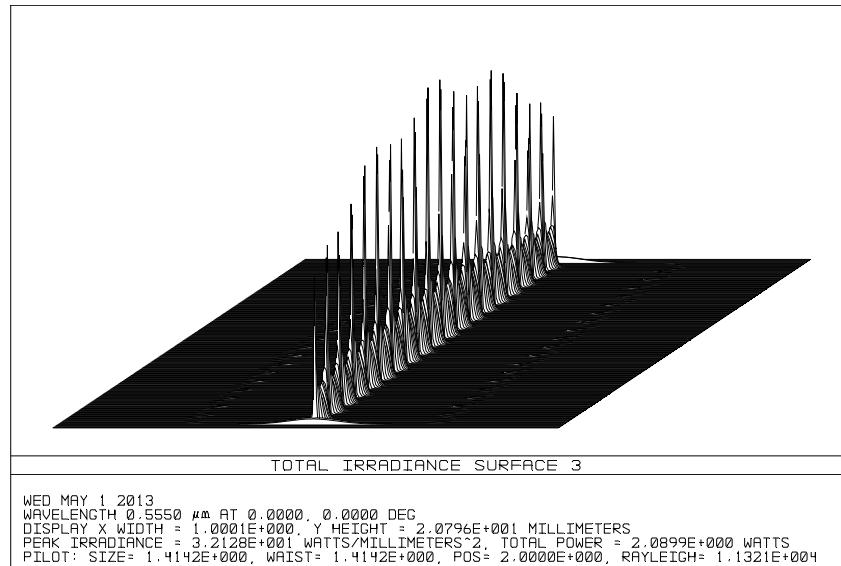


Figure-7. Irradiance distribution at overall slice in 3 dimension.

In 2-D plano-convex microlens array prototype; Figure-8 shows total irradiance distribution in image surface, which has peak irradiance of about 14 W/mm², this number represents amount of total irradiance that income the image surface. While Figure-9 shows X-cross section total irradiance distribution in image surface. It

seems slightly graduated power distribution by increasing from the center to edges of slice due to light diffraction. 3-D irradiance distribution in image surface has been illustrated in Figure-10. However, the optical system ensures roughly organized power distribution in all PVC's.

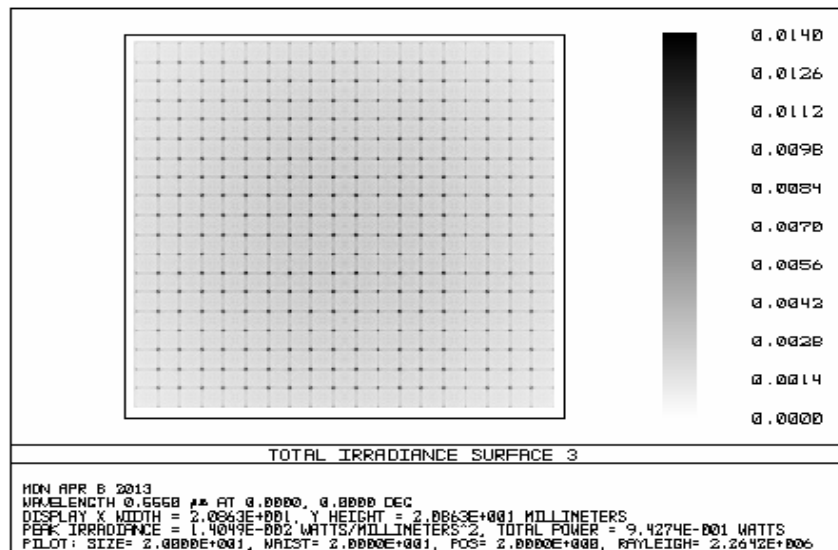


Figure-8. Total irradiance distribution in image surface.



www.arnjournals.com

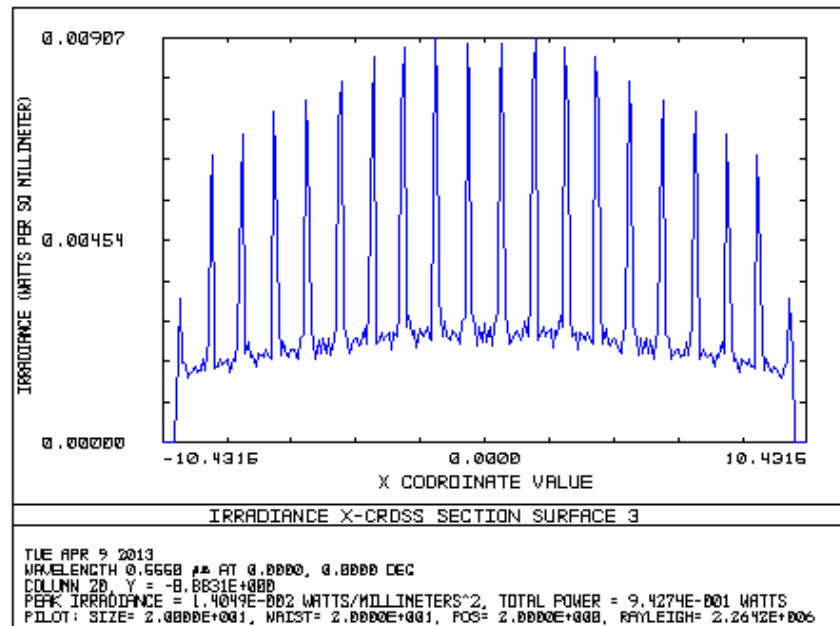


Figure-9. X-cross section of total irradiance distribution.

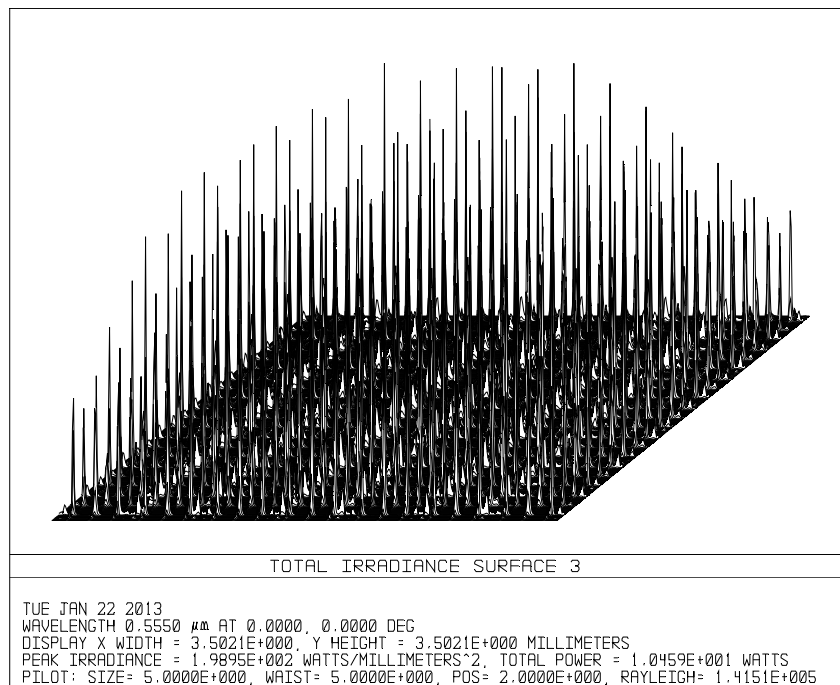


Figure-10. Total irradiance distribution in 3 dimensions.

In 2-D plano-convex microlens array with waveguide prototype; irradiance distribution has been evaluated by non sequential ray tracing in ZEMAX that use detector viewer to measure irradiance. Once ray data has been recorded on the detectors, data can be shown as Incoherent Irradiance, which equals the power per unit area as a function of spatial position on the detector. Figures 11 and 12 illustrate incoherent Irradiance versus

X- coordinate on the detector in double and single ray propagation samples respectively. The Figures show random irradiance distribution on the detector results from choosing random analysis rays which can not cover all surface of detector. In spite these samples give about 82% optical efficiency for double ray and 78% optical efficiency for single ray.



www.arnjournals.com

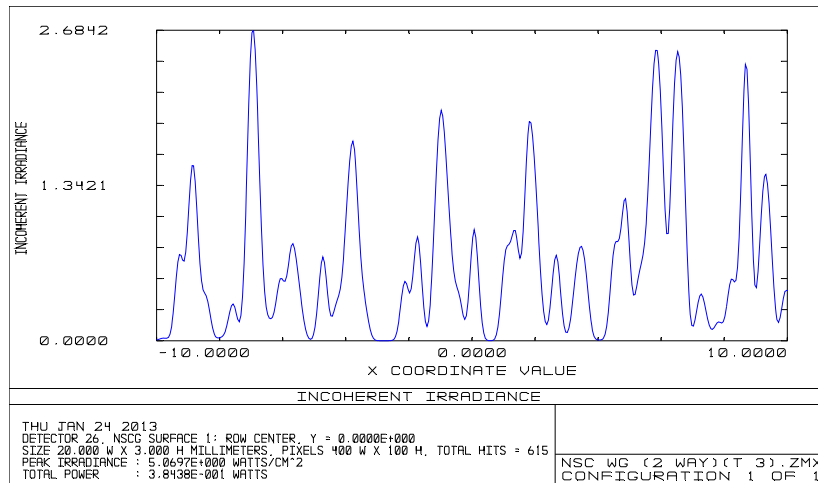
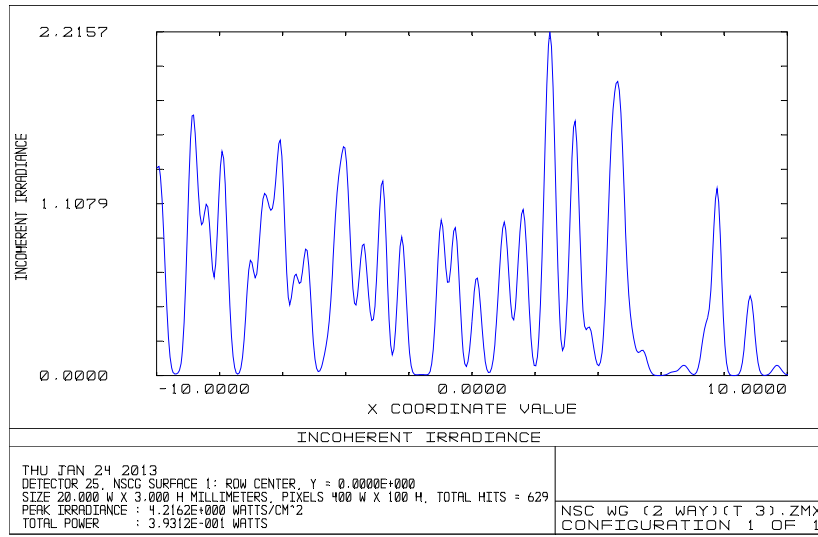


Figure-11. Incoherent irradiance versus X- coordinates in double ray propagation sample on the: A. detector 1, B. detector. 2.

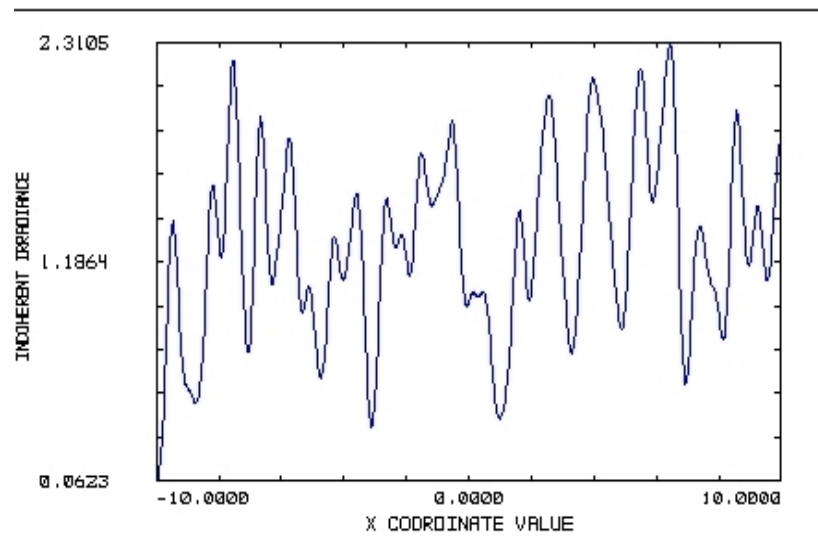


Figure-12. Incoherent irradiance versus X- coordinates in single ray propagation sample.



CONCLUSIONS

There are two methods to measure irradiance distribution in ZEMAX program: (1) sequential ray tracing mode to evaluate irradiance in 1-D and 2-D plano-convex microlens array prototypes. The prototypes illustrate slightly variation of irradiance distribution in the slice due to light diffraction. However, the optical system ensures roughly organized power distribution in all PVC's, (2) nonsequential ray tracing mode to evaluate irradiance in 2-D plano-convex microlens array with slab waveguide prototype. The prototype shows random irradiance distribution on the detector results from choosing random analysis rays which can not cover all surface of detector.

REFERENCES

- [1] Q. Volker. Technology fundamentals, the sun as an energy resource. *Renewable Energy World*. 6(5): 90-93.
- [2] R. Barakat and M. Morello. 1964. Computation of the Total Illuminance of an Optical System from the Design Data for Rotationally Symmetric Aberrations. *J. Opt. Soc. Am.* 54(3): 235-240.
- [3] R. Willson and A. Mordvinov. 2003. Secular total solar irradiance trend during solar cycles. *Geophys. Res. Lett.* 5(3): 21-23.
- [4] A. Guechi, M. Chegaar and A. Merabet. 2011. Effect of Spectral Irradiance Distribution on the Performance of Solar Cells. *Acta Physica Polonica*. 120(6): 19-23.
- [5] F. Bason. 1999. Diffuse Solar Irradiance and Atmospheric Turbidity. *Soldata Instruments*. 24(5): 25-31.
- [6] Ali AlHamdani. 2013. Experimental and Theoretical Design for a new Array Micro-Lenses Silicon Solar Cell Concentrator. *ARPN Journal of Engineering and Applied Sciences*. 8(3): 169-172.
- [7] G. Kopp and J. Lean. 2011. A New, Lower Value of Total Solar Irradiance: Evidence and Climate Significance. *Geophys. Res. Lett.* 13(5): 33-41.
- [8] J. H. Karp, E. J. Tremblay and J. E. Ford. 2010. Radial Coupling Method for Orthogonal Concentration within Planar Micro-Optic Solar Collectors. *Proc. of SPIE*. 18(2): 22-32.
- [9] J. H. Karp, E. J. Tremblay and J. E. Ford. 2009. Planar micro-optic solar concentrator using multiple imaging lenses into a common slab waveguide. *Proc. of SPIE*. 7407(4): 1-11.